



Ordered structures formed by nematic topological defects and their transformation with changing the Euler characteristics

P. V. Dolganov , N. A. Spiridenko , and V. K. Dolganov

Osipyan Institute of Solid State Physics RAS, 142432 Chernogolovka, Moscow Region, Russia



(Received 20 February 2024; accepted 1 August 2024; published 27 August 2024)

Ordered chain structures from topological defects of opposite charges (“necklaces” of defects) were prepared and their dynamics and cooperative rearrangement were investigated. We studied topological defects in nematic films with change of the Euler characteristic induced by temperature. Topological defects emerged due to competing surface anchoring on the nematic-isotropic and nematic-solid interfaces. Transformation of the structure with a circular chain from topological defects to the structure with a single defect and then to a structure without defects takes place as the nematic geometry changes. The temporal evolution of the number of topological defects at their annihilation in the chains differs from coarsening in two-dimensional (2D) and 3D geometry.

DOI: [10.1103/PhysRevE.110.024703](https://doi.org/10.1103/PhysRevE.110.024703)

I. INTRODUCTION

Topological defects are usually formed when symmetry breaks during phase transition [1–6]. A single topological defect cannot be born or disappear without change of the topology of the system. Formation and behavior of topological defects can be classified using topology and a topological invariant, namely Euler characteristic χ that is defined using the cell complex as $\chi = a_0 - a_1 + a_2 - \dots$, where a_i is the number of cells of dimension i [7]. The Euler characteristic χ for the surface of a three-dimensional (3D) object can be calculated as $\chi = 2 - 2g$, where g is the genus of the object or the number of “handles” [7]. For a sphere with n removed isolated noncrossing regions another formula exists: $\chi = 2 - n$. The Poincaré-Hopf theorem establishes the relation between topology and physics of condensed matter. According to the Poincaré-Hopf theorem, on the surface with the vector field the total topological charge of defects $\sum s_j = S$ equals the Euler characteristic χ of the surface (index j numerates the defects) [6]. In contrast to many other areas of physics, for example cosmology or quantum field theory, topological defects in liquid crystals can be easily obtained and visualized. Defects are formed in the ordered field of nematic \mathbf{n} director [1]. The topological charge of a defect in a 2D ordered field is defined as the number of turns of the field on a closed contour around the defect [6]. Liquid crystals became classical media for investigation of topological defects. In recent years, there has been increased attention to the structures formed by defects and the dynamics of individual and collective behavior of topological defects. Experimental and theoretical studies of the defect dynamics were performed for the case of pair interaction of two defects of opposite and the same topological charges [8–11]. Another active direction of investigation is the collective behavior of topological defects, the study of the time dependence of a dense array of disordered defects with attractive and repulsive forces in the 2D geometry (topological defect coarsening [9,12–23]). A series of works has been

devoted to studies of inclusions and liquid crystal droplets with nonspherical geometry. Many-handle particles and inclusions with various topologies have been obtained, topological transitions with a change of Euler characteristic and number of topological defects were investigated [24–28]. The field of molecular ordering and birth of topological defects at contact of several toroidal particles have been studied. A single torus has one handle and zero Euler characteristic. A particle composed by $g > 1$ tori has negative Euler characteristic $\chi = 2 - 2g$ and negative total topological charge of surface defects. A useful method for preparing toroids is injection of liquid or liquid crystal material into a rotating bath of yield stress material [29–31]. In such a way it is possible to create toroidal structures and conserve them for a long time. In nematic toroidal droplets $+1$ and -1 defect pairs located near the outer and inner parts of the torus were observed [31]. Defect pairs were created at the isotropic-nematic phase transition and correspond to a metastable state. The total topological charge of the defects in the torus was zero in accordance with topology [31]. In a number of studies ordered structures of topological defects were created by employing special techniques such as modulating the topography of the substrate, photopatterning, using laser tweezers and application of electric field [32–39]. These works suggest potential of practical application.

In our paper, ordered arrays from topological defects containing more than 10^2 defects organized in round chains (“necklaces” from topological defects) were prepared in nematic liquid crystal. Chains of defects obtained in our work form as a result of self-organization without employing special techniques. The end effects in the necklace are eliminated due to the formation of a closed round chain. Static and collective dynamics of obtained structures were investigated. We demonstrate the mechanism of formation of a point topological defect induced by change of the thickness of nematic film. We report topological transitions from a droplet touching the two surfaces of the cell to a droplet topologically equivalent to a semisphere and then to a toruslike structure with change

of the Euler characteristic χ and S from 0 to +1 and then to 0. Change of topological charges of defects S correlates with topological predictions. Previous studies have shown that 2D topological defect coarsening is characterized by power-law dependence of the number of defects from time $N(t) \sim t^{-\alpha}$, where α is 0.9–1 [13,15,17,18,22,23]. We found an essentially slower annihilation rate for our system.

II. EXPERIMENT

In our investigations nematic liquid crystal E7 (Synton Chemical) was used with a wide biphasic nematic-isotropic range about 2 K. This allows preparing isotropic droplets in the nematic environment and a large number of topological defects on the droplet interface. Nematic liquid crystal was in optical cells with a gap of thickness h about 40 μm . The extension of investigated isotropic droplets in the cell plane is much larger than h . We used homemade cells with coating favoring homeotropic orientation, that is, with the \mathbf{n} director perpendicular to the surfaces of the cells. For investigation of topological defects, a polarizing optical microscope (Olympus BX51) was used in the transmission mode. The cell was placed into a Linkam LTS120 thermostating stage. The dynamics of defects and their annihilation were monitored using a high-speed video camera (Baumer VCXU-02C).

III. RESULTS AND DISCUSSION

A large number of topological defects in 2D geometry is usually created by means of very fast cooling, mechanical or electric field influence on liquid crystal materials [17,22,23]. In our experiments we were successful in preparing a large array of topological defects in the form of a circular chain using a different procedure, namely, very slow cooling of a liquid droplet. Circular chains from topological defects were formed at the nematic-isotropic liquid interface in the two-phase nematic-isotropic region. To prepare the chains, large isotropic droplets with a diameter of several hundreds of microns in the nematic environment were first obtained by heating the nematic film [Fig. 1(a)]. Such droplets touch both surfaces of the cell (top and bottom). Their boundary is equivalent to a sphere with two removed noncrossing regions. Its Euler characteristic is $\chi = 2 - n = 0$, and $S = 0$. After preparing the droplet, heating was stopped and the sample was slowly cooled with a rate 0.1–0.2 $^{\circ}\text{C}/\text{min}$. Upon cooling to about 57 $^{\circ}\text{C}$ a thin circular stripe of the nematic phase was formed between the boundary of the cell and the surface of the isotropic droplet. Since in liquid crystal biphenyls and in mixture E7 the nematic \mathbf{n} director tilts with respect to the nematic-isotropic interface with azimuthal degeneracy [40,41] and orients perpendicular to the boundary of the cell with homeotropic anchoring (hybrid aligned liquid crystal), topological defects appear in the nematic stripe. Such defects form a circular chain (a necklace from topological defects). Typical examples of the chains from defects are shown in Figs. 1(b) and 2(a). Figure 1(c) shows two adjacent topological defects on a large scale. The projection of the \mathbf{n} director on the isotropic-nematic interface can be considered as the 2D director field.

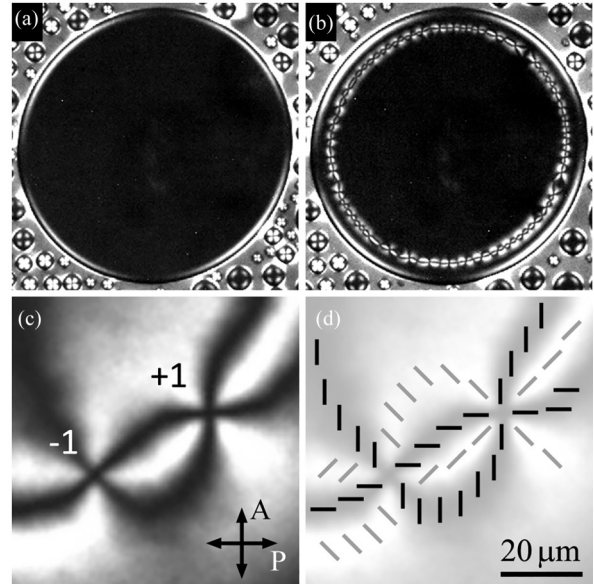


FIG. 1. (a) A large isotropic droplet (black area in crossed polarizers) in nematic environment. Small isotropic droplets are also present in the nematic film. (b) A circular chain of topological defects appeared in confined geometry of isotropic droplet. (c) Two topological defects of opposite signs ($s = +1$ and $s = -1$) from the chain. The projection of the \mathbf{n} director onto the nematic-isotropic interface forms an ordered field on the interface. This field is shown in (d). Orientation of crossed polarizer (P) and analyzer (A) is shown. The scale bar is given for frames (c) and (d). The horizontal size of frames (a) and (b) is 850 μm .

We start with the description of the static structure and dynamic transformation of chains [Figs. 1(b) and 2(a)]. When viewed in crossed polarizers, four dark and four bright brushes extend from each defect. This means that the module of the topological charge of every defect $|s_j| = 1$. Types of topological defects and their topological charges were determined using different orientation of polarizers and a Berek compensator. A part of the chain [Fig. 2(a)] is shown in Figs. 2(b)–2(d) in large scale. When the sample is viewed between vertical and horizontal crossed polarizers, the neighboring defects denoted A and B look the same [Fig. 2(b)]; the dark brushes in these defects are oriented nearly vertically and horizontally. We determine the sign of the topological charge by rotating the polarizers. Figure 2(d) shows the appearance of the same region when the polarizer P and analyzer A are both rotated in clockwise direction by 15 $^{\circ}$ with respect to Fig. 2(b). The reaction of the extinction pattern of defects A and B to polarizer rotation is different. The brushes of defect A rotate in opposite direction with respect to polarizers (counterclockwise) and the brushes of defect B rotate in the same direction as the polarizers (clockwise). This indicates that the topological charge of defect A is -1 and the charge of defect B is $+1$ [2]. In the chains the topological charge of neighboring defects is found to be the opposite. So the chain is composed by alternating $+1$ and -1 defects. The number of topological defects N in a closed chain is even [for example, in the chain in Fig. 2(a), $N = 42$], and the total topological charge of the chain is zero. There are two types of $+1$

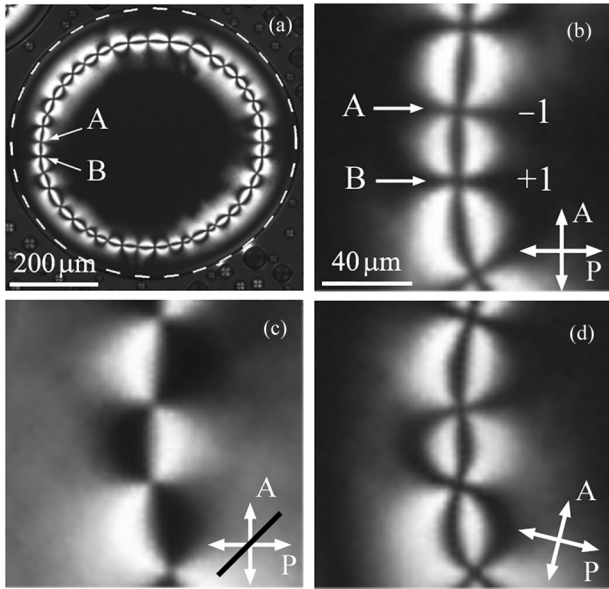


FIG. 2. (a) A circular chain (necklace from topological defects) formed in a circular nematic stripe on the periphery of isotropic droplet. The boundary of the droplet is indicated by a thin dashed line. (b)–(d) The region with two defects denoted A and B in frame (a) is shown on an enlarged scale with different orientation of polarizers (b),(d) and with a Berek compensator (c). (b) Crossed polarizers are oriented parallel and perpendicular to the segment of the chain. (c) View with a Berek compensator (the slow axis of the compensator is shown by the dark line). (d) The polarizer and the analyzer are rotated by 15° clockwise with respect to (b). The brushes of the defect B rotate in the same direction (clockwise), the brushes of defect A rotate in the opposite direction (counterclockwise). The type of defect (+1, -1) is shown in frame (b).

topological defects with radial and circular orientation of director around the center of defect [42]. The distribution of the director around +1 defects can be found from observations with the Berek compensator [Fig. 2(c)]. When a Berek compensator is inserted under 45° with respect to polarizers, the appearance of defects A and B differs: the positions of dark and bright regions around defects A and B are the opposite [Fig. 2(c)]. The pattern around defect B in Fig. 2(c) demonstrates that the director has a radial orientation [42]. Figure 1(d) shows schematically the orientation of the director field near two defects in the chain.

The peculiarities of formation of chain structure from defects are connected with topology of the system. Euler characteristic of a closed circle $\chi = 0$. So, according to Poincaré-Hopf theorem the sum of topological charges of the defects S must be zero ($S = 0$). In our experiments chains without distortions formed in different events have regular features. We found that number of topological defects in closed chains with different total numbers of defects and different size of the circle was even. We found that in closed chains (Figs. 2 and 3) in which we were able to determine the sign of the topological defects, the number of the topological defects with charge $s = +1$ equals the number of $s = -1$ defects. Defects with opposite charges alternate, so $S = 0$ as the topology predicts. After formation of a circular chain the

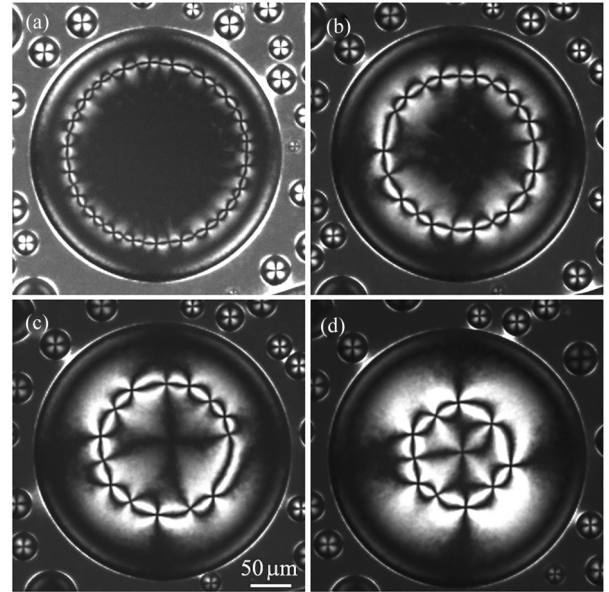


FIG. 3. Time evolution of the chain from topological defects at their annihilation. The number of the defects in the chain $N(t)$ and the radius of the chain decrease with time. When a thin nematic film is formed in the central area, $s = +1$ topological defect appears in the center (d). The total number of topological defects in the droplet becomes odd ($N = 11$). Time after frame (a) is 75 s (b), 160 s (c), and 270 s (d).

droplets in Figs. 1(b), 2(a), and 3(a) continue to touch the two surfaces of the cell (central region of the droplets), so their Euler characteristic can be calculated as $\chi = 2 - n = 0$.

At heating the round stripe with the chain of defects melts, the isotropic droplet increases in size, and all the film transforms in the isotropic phase. At small cooling and even at a constant temperature the chain also disappears but in a nontrivial way. Neighboring defects in the chain with opposite charges approach each other and annihilate by pairs. The number of defects in the chain decreases. The radius of the chain also decreases [Figs. 3(a)–3(d)] but S remains zero. On cooling the nematic film gradually spreads to the center and a point topological defect with four bright and dark brushes is formed in the center [Fig. 3(d)]. Measurements with different orientations of the polarizers show that the topological charge of the defect in the center is +1. The question could arise about the topological reason of formation of a single point topological defect. The nematic area spreads from the droplet perimeter to the center and, as clearly visible in Fig. 3(d), its Euler characteristic was changed. Now the nematic-isotropic interface becomes topologically equivalent to a semisphere (a sphere with one removed region). The Euler characteristic of such object $\chi = +1$. So, the total topological charge of defects in the droplet must be $S = +1$. But in the chain the sum of topological charges S remains 0. So, in accordance with topology an additional defect with charge $s = +1$ appears, which we indeed observe [Fig. 3(d)].

In the previous paragraph, we have described the topological reason of formation of a new +1 defect. The mechanism of the topological defect formation with a point singularity is of considerable interest and even a challenge for various

fields of science. We found unusual features in the appearance of the $s = +1$ point defect. When the nematic spreads to the center, first the black wide cross without visible point singularity is formed [Fig. 3(c)]. At the study of director transformation we made investigations with different orientation of polarizers and a Berek compensator as in the case of the chain (Fig. 2). Utilizing the compensator, we determined the optical path difference in various regions of the nematic film covering the droplet. These investigations show that the thinner part of the nematic film (Fig. 3) is near the center. The anchoring energy for homeotropic orientation at the solid surface is about 10^{-5} J/m² near the nematic-isotropic transition [1]. This value is substantially larger than the polar anchoring energy for the tilted orientation at the nematic-isotropic interface in cyanobiphenyls (about 5×10^{-7} J/m² in 4-cyano-4'-pentylbiphenyl (5CB) [1]). In very thin films the anchoring energy at the cell surface can dominate and nematic orientation is perpendicular to the cell plane. Similar director reorientation was observed in thin nematic cells with hybrid anchoring and different anchoring strength at the two solid surfaces [43,44]. On slow cooling, the nematic film becomes thicker and the \mathbf{n} director near the nematic-isotropic interface deviates from homeotropic orientation. The point singularity is gradually formed in the center [Fig. 3(d)]. The effective size of the central defect core in Fig. 3(d) determined from optical investigations is less than 3 μm . So, in our experiment we demonstrate how a topological defect with point singularity can continuously arise.

In some other measurements, in particular for higher rate of cooling, we observed the birth of several new defects in the central region. These defects are formed similar to a single defect described in the previous paragraph. The number of these new defects was always odd with sum of their topological charges $S = +1$. For instance, in the case of three new defects, two defects with $s = +1$ and one defect with $s = -1$ were born. Then the $s = -1$ defect annihilates with its antipode ($s = +1$ defect) and as a result only one $+1$ defect remains as in the case of Fig. 3(d).

In earlier investigations of the 2D dense arrays of topological defects [12–15,18,19] the main purpose was the studies of the collective behavior of defects, namely, the number of defects $N(t)$ or defect density $\rho(t)$ as a function of time when defects of opposite signs meet and annihilate in pairs. Theoretically two systems of particles and antiparticles were considered: (1) the particles and antiparticles move purely diffusively and annihilate at meeting in pairs ($+1$ and -1 defects); (2) defects move due to the long-range Coulomb forces between particles. The first model was considered by Toussaint and Wilczek [12]. They found that particle density as a function of time $\rho(t)$ strongly depends on the dimension D of system. For a one-dimensional model $\rho(t) \propto (t)^{-1/4}$. In space of dimension $D = 2$ the square root dependence on time $\rho(t) \propto (t)^{-1/2}$ was found. Jang *et al.* [18] numerically studied the evolution of the 2D system when diffusion motion dominates and obtained similar results (a power law with the exponent about -0.55). There is a large number of theoretical and experimental papers on the annihilation dynamics in 2D systems with opposite ($+1$, -1) charged defects [5,7,11,15,17]. For two defects of opposite charges the attractive force is $F \propto -K/L$, where K is the elastic constant

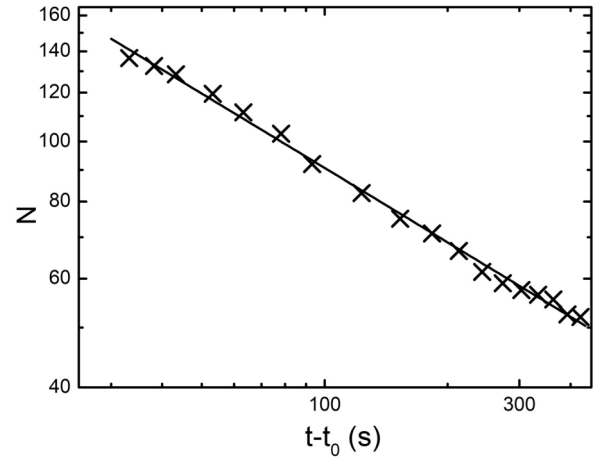


FIG. 4. The number of topological defects in the chains N versus time. The solid line is the power-law dependence $N(t) = A/(t - t_0)^\nu$ with an exponent $\nu = 0.4$.

and L is the separation between defects. For viscous liquid crystal the dissipation of energy is connected with the rotation of the director at the motion of the defect. The friction force F_f is $F_f \propto \eta \zeta dL/dt$, where $\zeta = \ln(R/R_c)$ [9,14], R is the size of the topological defect, R_c is its core radius, η is the damping constant (viscosity), and dL/dt is the velocity of the defect. On the basis on these two forces the equation of motion is $\zeta dL/dt \propto K/L\eta$ [9]. For the 2D space the scaling or the self-similarity argument was used to calculate $N(t)$ from time [9,22]. If at coarsening the system is characterized by the single length scale (average distance between defects) $r(t)$ the equation for $L(t)$ is valid for $r(t)$ [9]. The scaling solution of the differential equation gives $r^2(t) \propto t$ [9]. The number of defects at time t in the 2D system is $N(t) \approx A/r^2(t)$, where A is the area of the sample. So, the number of defects decay inverse to the time $N(t) \propto (t)^{-1}$.

Temporary dependence $N(t)$ in our experiment is shown in Fig. 4. In the analysis we used droplets with the initial number of defects in the chain $N \gtrsim 10^2$ and the radius about 400 μm . The dependence $N(t)$ can be described by power law $N(t) = A/(t - t_0)^\nu$ with an exponent $\nu = 0.4 \pm 0.1$. This value ν is essentially smaller than the exponent $\nu = 1$ obtained in scaling in the case of 2D topological defect annihilation and even than the exponent about 0.9 obtained in numerical calculations and in experiments [13,17,18,22,23]. The difference of our value with the existing data for 2D systems [13,17,18,22,23] can be connected with the difference of our system with 2D ones in previous experimental and theoretical investigations [13,17,18,22,23]. In experiments on 2D coarsening the area where $N(t)$ was determined remains the same. In our case the length of the chain $L(t)$ decreases with time, which should also lead to some decrease of the value of ν .

The circular chain exists when the distance between nearest defects is relatively small. The situation is changed when the number of defects in the chain becomes small and the distance between defects is of the order of radius of the chain. The chain becomes unstable, is destroyed, and all the defects form a single system with an odd number of defects. As the result

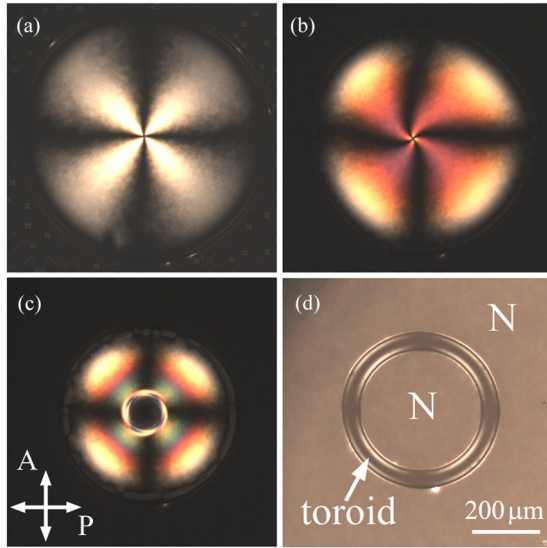


FIG. 5. Topological transition of an isotropic droplet with a point defect on the nematic-isotropic interface (a) to a toroid (d) without topological defects. (a),(b) Evolution of the topological defect on the nematic-isotropic interface. The interference colors change with increasing nematic thickness. (c) Formation of a nematic hole in the isotropic droplet. The hole starts to form in the center of the topological defect. (d) A toruslike droplet without topological defects on the nematic-isotropic interface. N denotes the nematic phase. The exposure time in frame (d) was increased with respect to frames (a)–(c). Time after frame (a) is 145 s (b), 315 s (c), and 470 s (d).

of their annihilation only one $+1$ topological defect remains [Fig. 5(a)]. In thin nematic film black brushes of the defect are oriented parallel and perpendicular to the polarizer and analyzer. At cooling the droplet transforms its shape. When the thickness of the nematic film increases bright brushes become colored [Fig. 5(b)] and brushes near the defect core somewhat rotate with respect to vertical and horizontal orientation [Fig. 5(b)]. This rotation can be connected with twist of the \mathbf{n} director around the axis perpendicular to the isotropic-nematic interface. We observed chiral structures in achiral nematic E7. Such chiral symmetry breaking was observed in thermotropic nematic and in achiral lyotropic chromonic liquid crystals [45–48]. Formation of these structures is related to spatial confinement and anisotropy of orientational elasticity, when the twist elastic constant is smaller than the bend and splay constants [45,48]. We observed rotation of brushes in different events both in clockwise and counterclockwise directions. Such equal probability of both handedness is due to the nonchiral liquid crystal [45,48].

At further cooling the center of the isotropic droplet is filled with a nematic crater [Fig. 5(c)], the defect disappears, and a circular liquid toroid, which is topologically equivalent to a torus, is formed in the nematic environment [Fig. 5(d)]. The Euler characteristic of the torus ($g = 1$) is $\chi = 0$. The torus-like droplet in Fig. 5(d) has no topological singularities which correlate with topology. It has been shown that depending on the aspect ratio R/a , where R is the central ring radius and a is the tube radius, and on the elastic anisotropy, the nematic director configuration inside the torus could be both chiral and nonchiral [46,49]. At large ratio R/a the configuration in the torus is nonchiral. In our case the torus is nonchiral [$R/a \approx 8$, Fig. 5(d)]. Further evolution of the torus can occur via breakup due to Rayleigh-Plateau instability at $R - a \gg a$ or via shrinkage towards the center when $R - a \ll a$ [29,30]. In our case at $(R - a)/a \approx 8.5$ we observed the breakup of the toroid with the appearance of small droplets.

Koizumi *et al.* [45] at heating observed transformation of a lyotropic nematic tactoid to a torus. They explained this transformation by the interplay of nematic elastic constants (splay K_{11} and bend K_{33} modulus) and hindrance of splay deformation in the torus. At the latest stage of our series of transformations we demonstrate the topological process at cooling and formation of isotropic toroid. The nematic hole in the droplet starts to form in the center of the topological defect [Fig. 5(c)]. This process with change of topology and decreasing χ leads to a small elastic deformation.

IV. SUMMARY

In our experiments, we have realized circular chains from defects of opposite topological charges (a necklace from defects) and investigated their collective dynamics. It was established that defect formation in the chain and defect annihilation are consistent with topological predictions. The mechanism of continuous formation of a point topological defect was demonstrated. In the chain the numbers of defects of opposite topological charges are equal, in the droplet topologically equivalent to a semisphere the number of $+1$ defects exceeds the number of -1 defects by 1, and the toruslike structure is formed without topological defects. We realized a transition from the droplet connecting two cell surfaces to the droplet topologically equivalent to a semisphere and then to toroidal droplet and found that defect transformation correlates with topological predictions.

ACKNOWLEDGMENT

The work was supported by the Russian Science Foundation (Project No. 23-12-00200).

The authors declare no conflict of interest.

- [1] M. Kleman and O. D. Lavrentovich, *Soft Matter Physics: An Introduction* (Springer, New York, 2003).
- [2] P. Oswald and P. Pieranski, *Nematic and Cholesteric Liquid Crystals* (Taylor & Francis, Boca Raton, 2005).
- [3] M. Kleman and O. D. Lavrentovich, Topological point defects in nematic liquid crystals, *Philos. Mag.* **86**, 4117 (2006).

- [4] P. M. Chaikin and T. S. Lubensky, *Principles of Condensed Matter Physics*, 7th ed. (Cambridge University Press, Cambridge, UK, 2013).
- [5] K. Harth and R. Stannarius, Topological point defects of liquid crystals in quasi-two-dimensional geometries, *Front. Phys.* **8**, 112 (2020).

- [6] S. Fumeron and B. Berche, Introduction to topological defects: From liquid crystals to particle physics, *Eur. Phys. J. Spec. Top.* **232**, 1813 (2023).
- [7] A. Hatcher, *Algebraic Topology* (Cambridge University Press, Cambridge, UK, 2002).
- [8] A. Pargellis, N. Turok, and B. Yurke, Monopole-antimonopole annihilation in a nematic liquid crystal, *Phys. Rev. Lett.* **67**, 1570 (1991).
- [9] B. Yurke, A. N. Pargellis, T. Kovacs, and D. A. Huse, Coarsening dynamics of XY model, *Phys. Rev. E* **47**, 1525 (1993).
- [10] R. Stannarius and K. Harth, Defect interaction in anisotropic two-dimensional fluid, *Phys. Rev. Lett.* **117**, 157801 (2016).
- [11] A. Missaoui, K. Harth, P. Salamon, and R. Stannarius, Annihilation of point defect pairs in freely suspended liquid-crystal films, *Phys. Rev. Res.* **2**, 013080 (2020).
- [12] D. Toussaint and F. Wilczek, Particle-antiparticle annihilation in diffusive motion, *J. Chem. Phys.* **78**, 2642 (1983).
- [13] R. Loft and T. A. DeGrand, Numerical simulation of dynamics in the XY model, *Phys. Rev. B* **35**, 8528 (1987).
- [14] H. Pleiner, Dynamics of a disclination point in smectic-*C* and -*C* liquid-crystal films, *Phys. Rev. A* **37**, 3986 (1988).
- [15] H. Toyoki, Pair annihilation of point like topological defects in the ordering process of quenched systems, *Phys. Rev. A* **42**, 911 (1990).
- [16] G. Ryskin and M. Kremenetsky, Drag force on a line defect moving through an otherwise undisturbed field: Disclination line in a nematic liquid crystal, *Phys. Rev. Lett.* **67**, 1574 (1991).
- [17] T. Nagaya, H. Hotta, H. Orihara, and Y. Ishibashi, Experimental study of the coarsening dynamics of +1 and -1 disclinations, *J. Phys. Soc. Jpn.* **61**, 3511 (1992).
- [18] W. G. Jang, V. V. Ginzburg, C. D. Muzny, and N. A. Clark, Annihilation rate and scaling in two-dimensional system of charged particles, *Phys. Rev. E* **51**, 411 (1995).
- [19] V. V. Ginzburg, P. D. Beale, and N. A. Clark, Scaling theory of particle annihilation in system with long-range interaction, *Phys. Rev. E* **52**, 2583 (1995).
- [20] C. Liu and M. Muthukumar, Annihilation kinetics of liquid crystal defects, *J. Chem. Phys.* **106**, 7822 (1997).
- [21] I. Dierking, O. Marshall, J. Wright, and N. Bulleid, Annihilation dynamics of umbilical defects in nematic liquid crystal under applied electric field, *Phys. Rev. E* **71**, 061709 (2005).
- [22] V. Zambra, M. G. Clerc, R. Barboza, U. Bortolozzo, and S. Residori, Umbilical defect dynamics in an inhomogeneous nematic liquid crystal layer, *Phys. Rev. E* **101**, 062704 (2020).
- [23] R. A. Chowdhury, A. A. S. Green, C. S. Park, J. E. Maclennan, and N. A. Clark, Topological defect coarsening in quenched smectic-*C* films analyzed using artificial neural networks, *Phys. Rev. E* **107**, 044701 (2023).
- [24] I. I. Smalyukh, Y. Lansac, N. A. Clark, and R. P. Trivedi, Three-dimensional structure and multistable optical switching of triple-twisted particle-like excitations in anisotropic fluids, *Nat. Mater.* **9**, 139 (2009).
- [25] B. Senyuk, O. Liu, S. He, R. D. Kamien, T. C. Lubensky, and I. I. Smalyukh, Topological colloids, *Nature (London)* **493**, 200 (2013).
- [26] U. Tkalec and I. Muševič, Topology of nematic liquid crystal colloids confined to two dimensions, *Soft Matter* **9**, 8140 (2013).
- [27] E. Pairam, J. Vallamkondu, V. Koning, B. C. van Zuiden, P. W. Ellis, M. A. Bates, V. Vitelli, and A. Fernandez-Nieves, Stable nematic droplets with handles, *Proc. Natl. Acad. Sci. USA* **110**, 9295 (2013).
- [28] Y. Yuan, P. Keller, and I. I. Smalyukh, Elastomeric nematic colloids, colloidal crystals and microstructures with complex topology, *Soft Matter* **17**, 3037 (2021).
- [29] E. Pairam and A. Fernandez-Nieves, Generation and stability of toroidal droplets in a viscous liquid, *Phys. Rev. Lett.* **102**, 234501 (2009).
- [30] E. Pairam, H. Le, and A. Fernández-Nieves, Stability of toroidal droplets inside yield stress materials, *Phys. Rev. E* **90**, 021002(R) (2014).
- [31] J. Rojo-González, L. N. Carezza, A. de la Cotte, L. A. Hoffmann, L. Giomi, and A. Fernandez-Nieves, Defect-populated configurations in nematic solid tori and cylinders, *Phys. Rev. Res.* **6**, L012065 (2024).
- [32] M. Cavallaro, Jr., M. A. Gharbi, D. A. Beller, S. Čopar, Z. Shi, T. Baumgart, S. Yang, R. D. Kamien, and K. J. Stebe, Exploiting imperfections in the bulk to direct assembly of surface colloids, *Proc. Natl. Acad. Sci. USA* **110**, 18804 (2013).
- [33] Y. Sasaki, V. S. R. Jampani, C. Tanaka, N. Sakurai, S. Sakane, K. V. Le, F. Araoka, and H. Orihara, Large-scale self-organization of reconfigurable topological defect networks in nematic liquid crystals, *Nat. Commun.* **7**, 13238 (2016).
- [34] M. Wang, Y. Li, and H. Yokoyama, Artificial web of disclination lines in nematic liquid crystals, *Nat. Commun.* **8**, 388 (2017).
- [35] P. Salamon, N. Éber, Y. Sasaki, H. Orihara, Á. Buka, and F. Araoka, Tunable optical vortices generated by self-assembled defect structures in nematics, *Phys. Rev. Appl.* **10**, 044008 (2018).
- [36] D. S. Kim, S. Čopar, U. Tkalec, and D. K. Yoon, Mosaics of topological defects in micropatterned liquid crystal textures, *Sci. Adv.* **4**, eaau8064 (2018).
- [37] M. S. Kim and F. Serra, Tunable dynamic topological defect pattern formation in nematic liquid crystals, *Adv. Opt. Mater.* **8**, 1900991 (2020).
- [38] Y. Guo, M. Jiang, S. Afghah, C. Peng, R. L. B. Selinger, O. D. Lavrentovich, and Q.-H. We, Photopatterned designer disclination networks in nematic liquid crystals, *Adv. Opt. Mater.* **9**, 2100181 (2021).
- [39] S.-B. Wu, J.-B. Wu, H.-M. Cao, Y.-Q. Lu, and W. Hu, Topological defect guided order evolution across the nematic-smectic phase transition, *Phys. Rev. Lett.* **130**, 078101 (2023).
- [40] S. Faetti and V. Palleschi, Nematic-Isotropic interface of some members of the homologous series of 4-cyano-4'-(*n*-alkyl)biphenyl liquid crystals, *Phys. Rev. A* **30**, 3241 (1984).
- [41] Y. K. Kim, S. V. Shiyakovskii, and O. D. Lavrentovich, Morphogenesis of defects and tactoids during isotropic-nematic phase transition in self-assembled lyotropic chromonic liquid crystals, *J. Phys.: Condens. Matter* **25**, 404202 (2013).
- [42] O. D. Lavrentovich, Looking at the world through liquid crystal glasses, *Contemp. Math.* **577**, 25 (2012).
- [43] G. Barbero, N. V. Madhusudana, and G. Durand, Anchoring energy for nematic liquid crystals an analysis of the proposed forms, *Z. Naturforsch.* **39a**, 1066 (1984).
- [44] M. Ruths and B. Zappone, Direct nematomechanical measurement of an anchoring transition in a nematic liquid crystal

- subject to hybrid anchoring conditions, [Langmuir](#) **28**, 8371 (2012).
- [45] L. Tortora and O. D. Lavrentovich, Chiral symmetry breaking by spatial confinement in tactoidal droplets of lyotropic cholesteric liquid crystals, [Proc. Natl. Acad. Sci. USA](#) **108**, 5163 (2011).
- [46] P. W. Ellis, K. Nayani, J. P. McInerney, D. Z. Rocklin, J. O. Park, M. Srinivasarao, E. A. Matsumoto, and A. Fernandez-Nieves, Curvature-induced twist in homeotropic nematic tori, [Phys. Rev. Lett.](#) **121**, 247803 (2018).
- [47] R. Koizumi, D. Golovaty, A. Alqarni, B. Li, P. J. Sternberg, and O. D. Lavrentovich, Topological transformations of a nematic drop, [Sci. Adv.](#) **9**, eadf3385 (2023).
- [48] J. Kim and J. Jeong, Confinement twists achiral liquid crystals and causes chiral liquid crystals to twist in the opposite handedness: Cases in and around sessile droplets, [Soft Matter](#) **20**, 1361 (2024), and references therein.
- [49] I. M. Kulic, D. Andrienko, and M. Deserno, Twist-bend instability for toroidal DNA condensates, [Europhys. Lett.](#) **67**, 418 (2004).